Supporting information for

A mechanistic investigation of dehalogenation using ESI-MS

Zohrab Ahmadi and J. Scott McIndoe

Experimental details

All syntheses and catalytic reactions were performed under an inert atmosphere of N_2 or Ar using standard glovebox or Schlenk procedures. The aryl iodide [4-$IC_6H_4CH_2PPh_3$][PF_6] and [Ph_3PMe][PF_6] were prepared by a literature method.[1] All chemicals were obtained from Aldrich and used without further purification. Solvents were HPLC grade and purified on an MBraun solvent purification system. Gases were obtained from Airgas (Calgary, Canada). All mass spectra were collected on a Micromass Q-ToF *micro* mass spectrometer in positive ion mode using pneumatically assisted electrospray ionization. Capillary voltage: 2900 V. Cone voltage: 10 V. Extraction voltage: 0.5 V. Source temperature: 70°C. Desolvation temperature: 150°C. Cone gas flow: 100 L/h. Desolvation gas flow: 100 L/h. Collision voltage: 2 V (for MS experiments). Collision voltage: 10-25 V (for MS/MS experiments). During PSI experiments, overpressure in the flask was held at 2.5 psi Ar throughout the reaction and the temperature was controlled by a digital thermometer mounted inside the flask. The reaction mixture was transferred to MS without further dilution through PEEK tubing (200 mm in length, i.d. 0.055 mm). Data was processed without any normalization for Eyring plots, but all other plots were normalized after applying a correction for variable ionization efficiency (dividing the measured response factors of each species including ArI (Ar = [4-$C_6H_4CH_2PPh_3$][PF_6]), ArH, Ar-Ar and observed intermediates over sum of all tag containing species). About 3600 spectra were collected per hour of monitoring (1 s^{-1}). For the monitoring 10 ml of 0.5 mM ArI in methanol was degassed and transferred to a Schlenk flask with integrated condenser and 2 mg of [Ph_3PMe][PF_6] added as the internal standard. 6% Pd(PPh_3)$_4$ (2 mL, 17 µM stock catalyst in THF) was added by syringe through the septum to initiate the reaction. The tetrakistriphenylphosphine palladium stock solution was stored in an inert atmosphere glovebox at -32°C between uses. Potassium *tert*-butoxide (10 equivalents, stock solution in MeOH) was added by syringe through the septum after addition of catalyst solution. For the reaction using excess iodide, 1 equivalent (to ArI) of [Ph_3PMe][I] was added as the source of iodide. For silver ion experiment, 1 equivalent (to ArI) $AgNO_3$ was added.

Numerical Modeling

Numerical modeling was performed using Powersim.[2] Colors are the same in all figures/schemes. Concentrations of intermediates are multiplied by 100 in the experimental plot but by 20 in the simulation; as we don't know the relative response factor for the intermediates vs. the substrate, we have paid attention to the relative abundances between intermediates and changes with time rather than the absolute abundances. The initial experimental concentrations were used as initial conditions. Units are min^{-1} for first order rate constants and $mM^{-1}\ min^{-1}$ for second order rate constants. Reverse reactions were considered in every single step for the flexibility purpose in the model. However the rate constants were considered as zero for those steps which are known to be effectively non reversible (reductive elimination and beta hydride elimination). For the CH_3OD experiment the deprotonation and protonation steps were slowed 16 times to match with experimental data (based on primary KIE and tunneling) and for the reaction in CD_3OD other than deprotonation step (same factor as CH_3OD: 16 time), the beta hydride elimination step was slowed down by a factor of 7. For the iodide addition experiment, 0.5 mM iodide (1 equivalent) was used as the starting concentration (Scheme S1). For Ag^+ addition, a new model including the involvement of the fast irreversible reaction between Ag^+ and I^- was considered in simulation Scheme S2. Table S1 shows the rate constants of different steps in all simulated reactions. Fig S(1-4) show the experimental and simulated graphs for each reaction.
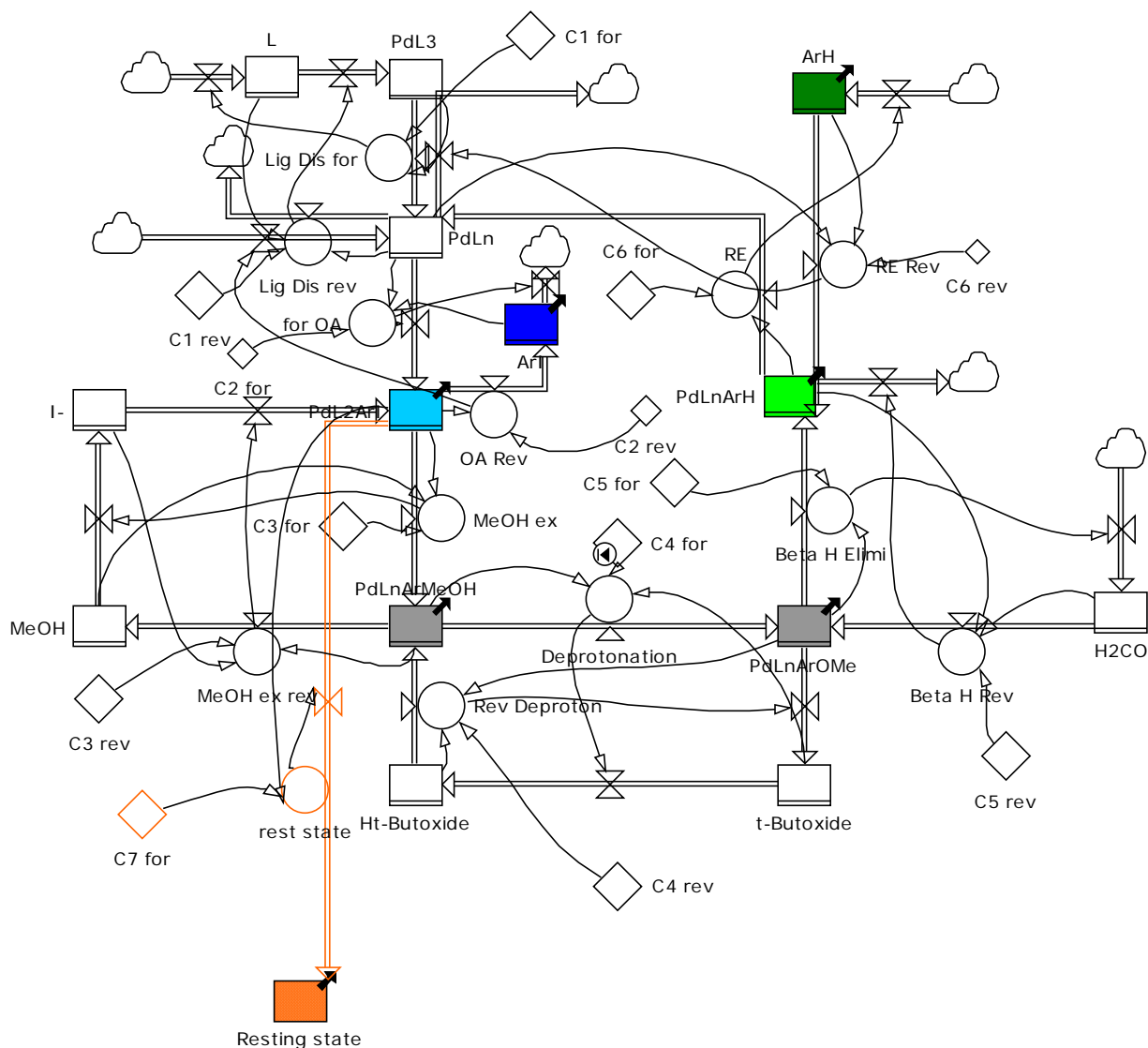
Scheme S1. Numerical model of hydrodehalogenation (applied for the reactions in MeOH, CH$_3$OD, CD$_3$OD and iodide addition).
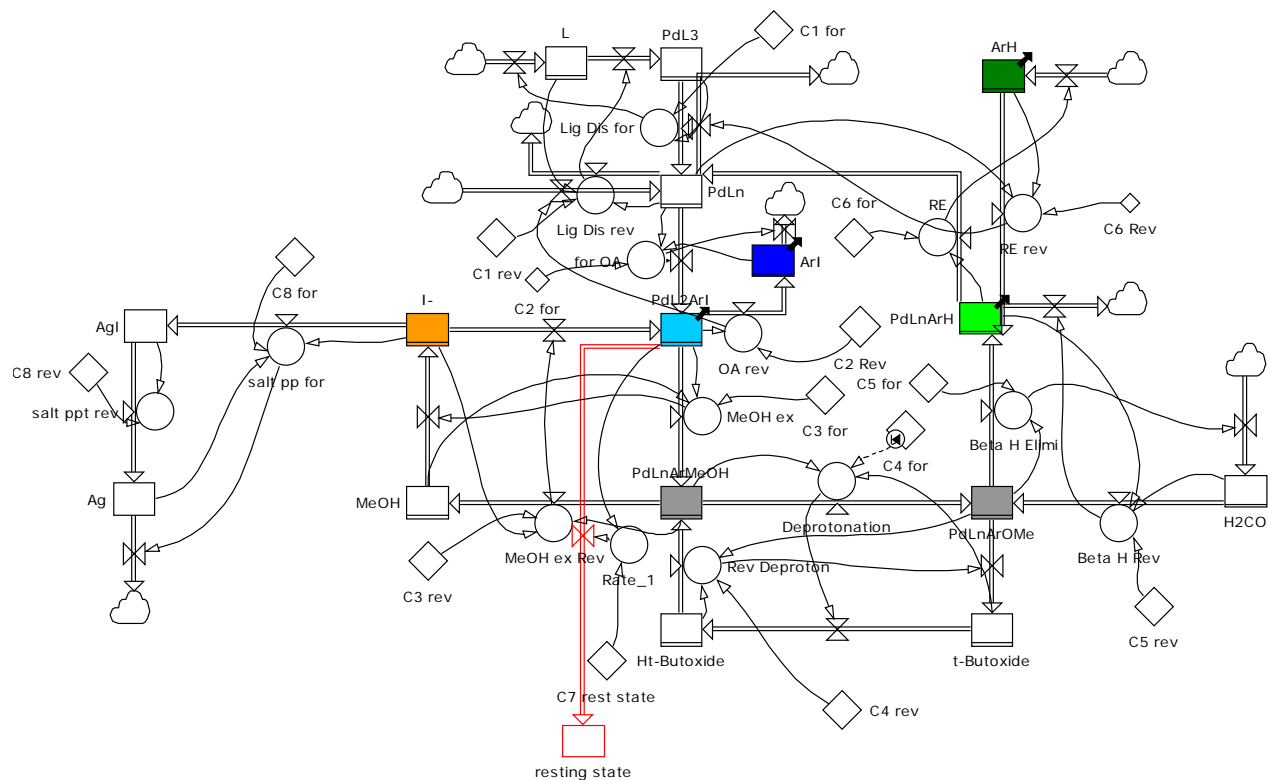
Scheme S2. Numerical model of hydrodehalogenation including Ag$^+$ reaction with I$^-$.

Table S1: Rate constant values in different experiments.

Rate constants	Experiments				
	MeOH	**MeOH-D1**	**MeOH-D4**	**Iodide**	**Ag$^+$**
C1 for	10,000	10,000	10,000	10,000	10,000
C1 rev	10,000	10,000	10,000	10,000	10,000
C2 for	1000	1000	1000	1000	1000
C2 rev	0	0	0	0	0
C3 for	1	1	1	1	1
C3 rev	3500	3500	3500	3500	3500
C4 for	0.6	0.04	0.04	0.6	0.6
C4 rev	100	6.25	6.25	100	100
C5 for	2000	2000	285	2000	2000
C5 rev	0	0	0	0	0
C6 for	1	1	1	1	1
C6 rev	0	0	0	0	0
C7 for	0.012	0.012	0.012	0.012	0.012
C8 for	-	-	-	-	1
C8 rev	-	-	-	-	0
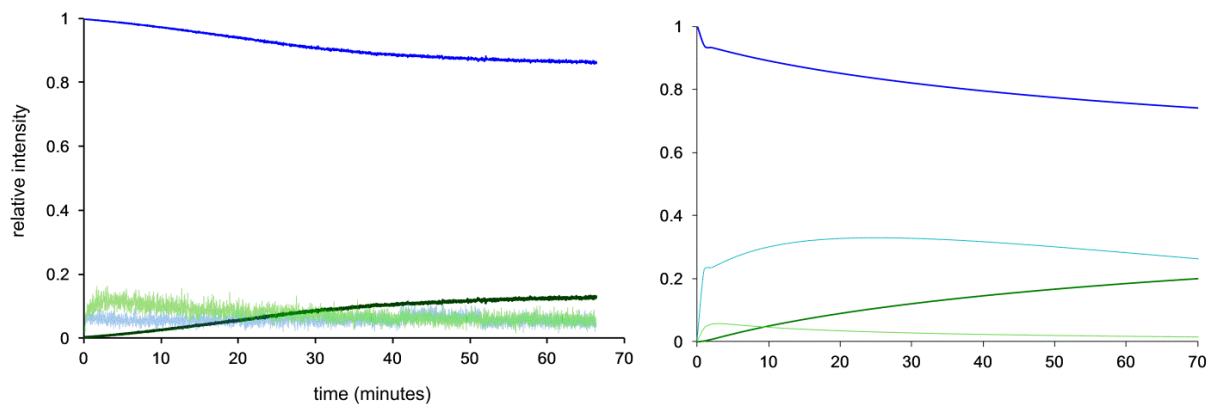
Figure S1: Reaction progress in CH_3OD: experimental (left) and numerically modeled using Powersim (right), under standard conditions.
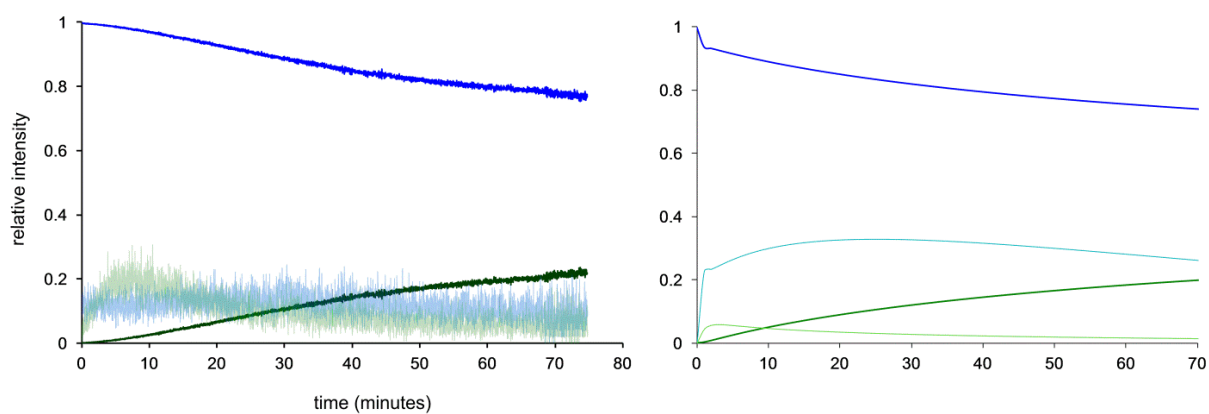
Figure S2: Reaction progress in CD_3OD: experimental (left) and numerically modeled using Powersim (right), under standard conditions.
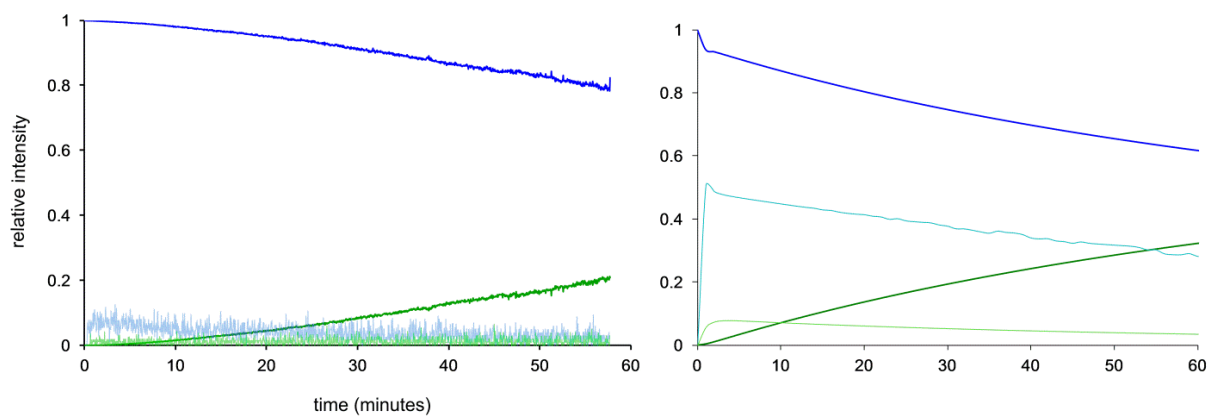
Figure S3: Reaction progress in CH_3OH with addition of 1 equivalent I^-: experimental (left) and numerically modeled using Powersim (right), under standard conditions.
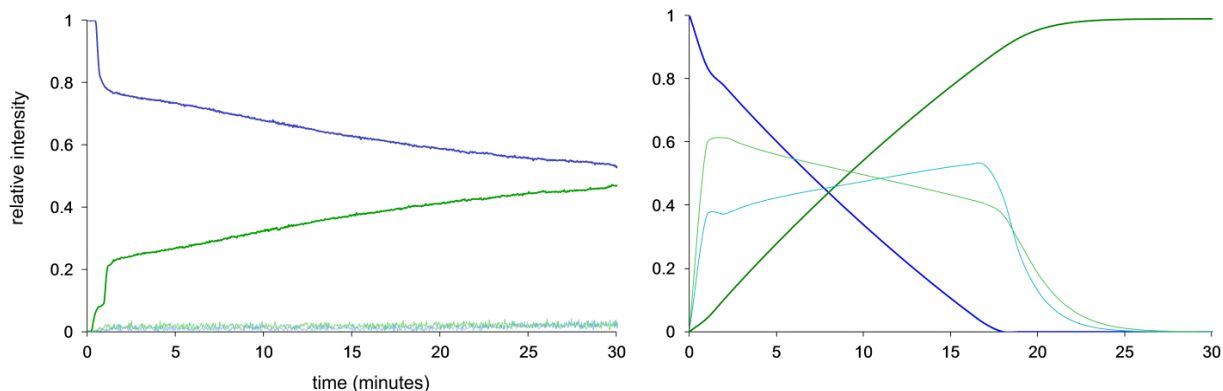
Figure S4: Reaction progress in CH_3OH with addition of 1 equivalent Ag^+: experimental (left) and numerically modeled using Powersim (right), under standard conditions.
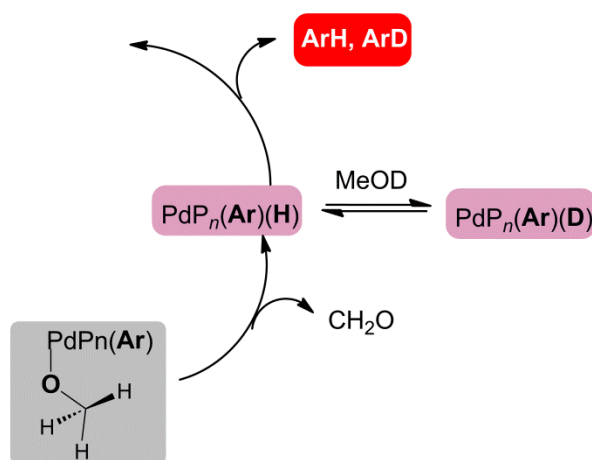
Scheme S3: H/D exchange and formation of a mixture of products in the CH_3OD. The fact that ArD is observed in the presence of CH_3OD suggests that D replaces H in PdL_2ArH. This assumption is reasonable since reductive elimination is slow and provides the chance for this exchange.
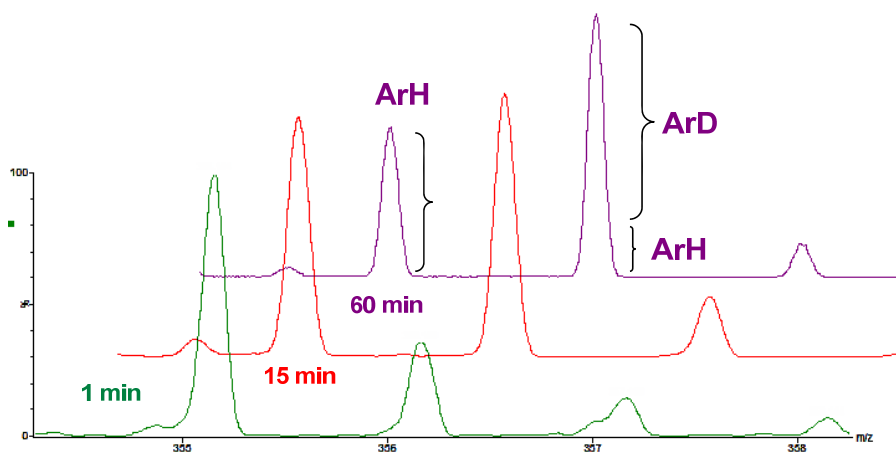
Figure S5: Formation of ArD over the course of reaction in CH_3OD. Note that initially ArH is the dominant product and ArD formation competes with that over the course of reaction.

6

In order to see if the perturbation made in the dehalogenation experiment (reaction in CH$_3$OD) can be reproduced in the postulated off-metal deprotonation of MeOH cycle, a model was constructed and optimized to match with traces in the MeOH (Scheme S4 and Figure S6). Afterwards, deprotonation of MeOH was slowed down between 7-16 (Normal KIE up to tunneling mechanism) in both directions. However, this change did not slow down the reaction rate.
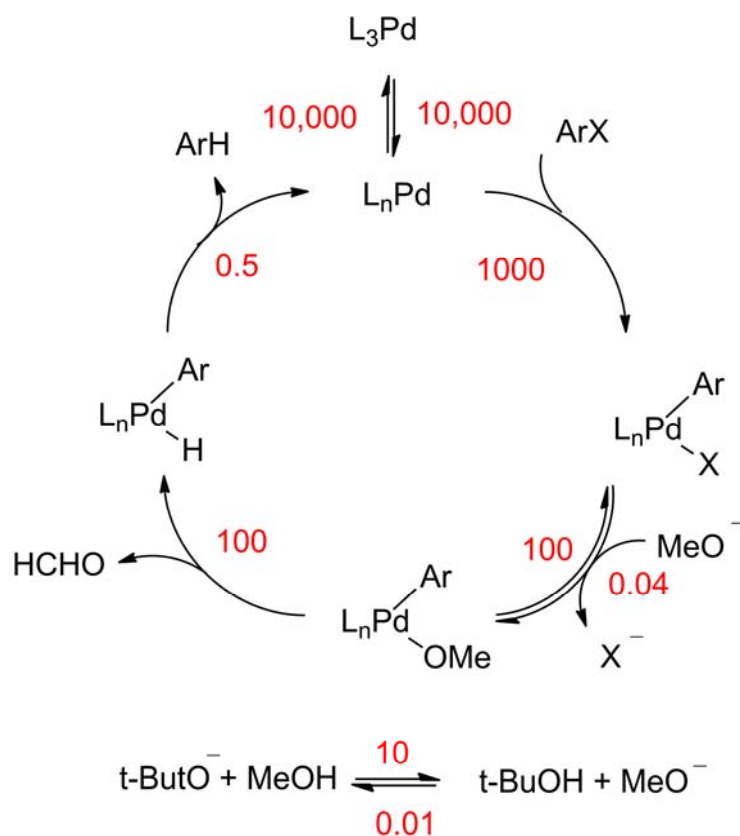
Scheme S4: Extracted rate constants for the conceivable off-metal deprotonation of MeOH in hydrodehalogenation which respond closely to observed traces of the experimental data (Figure S6). However, slowing down the deprotonation equilibrium in both directions failed to produce the observed traces in deuterated MeOH.
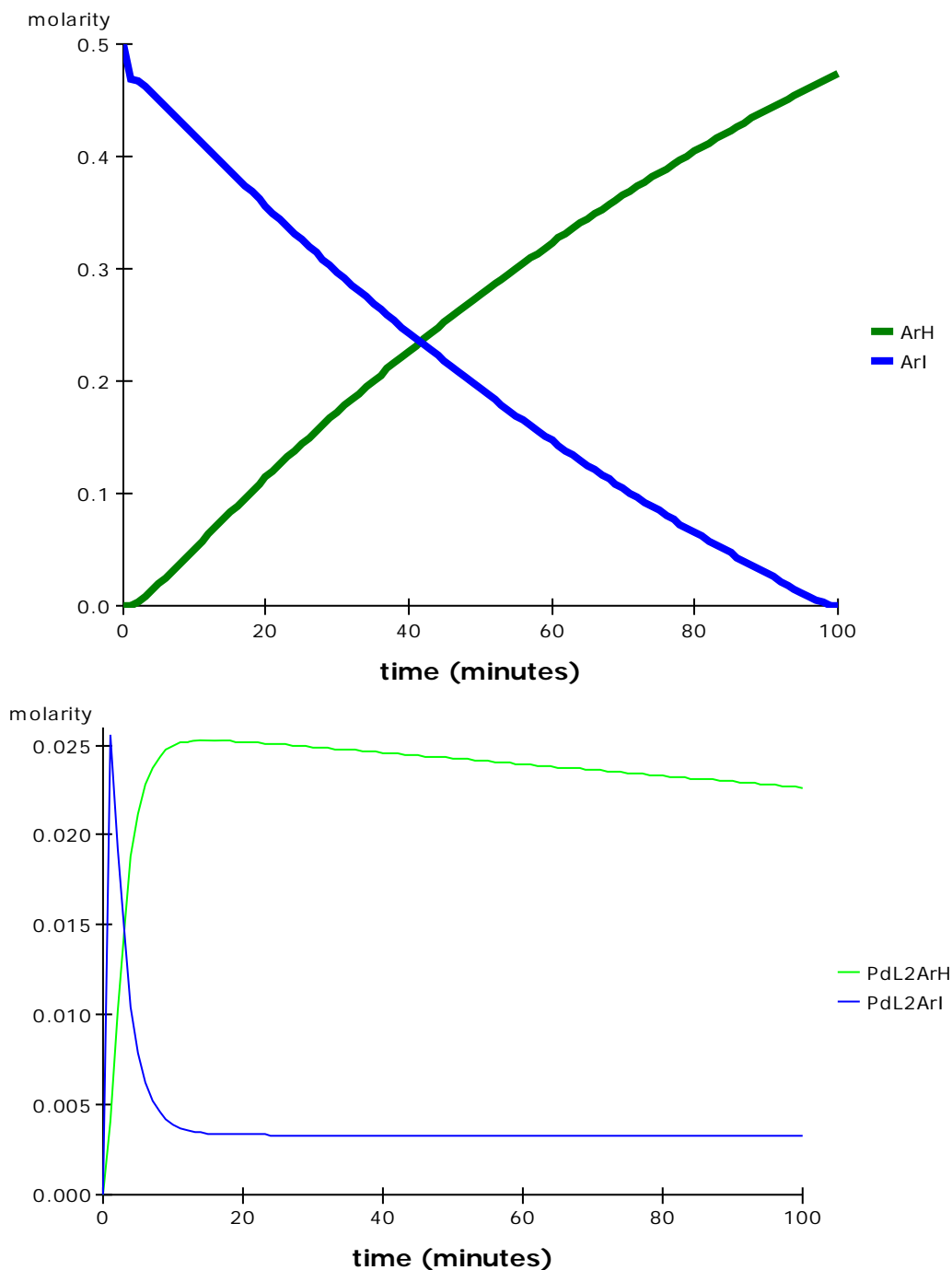
Figure S6: Simulated traces of the hydrodehalogenation in the MeOH using the rate constants shown in Scheme S4. (top). Traces of ArI and ArH (bottom) traces of the intermediates; PdL$_2$ArH and PdL$_2$ArI.

Observation of hidden intermediate

Proposed mechanism for hydrodehalogenation as well as numerical model suggests that $[PdL_2Ar(MeOH)]^{2+}$ or $[PdL_2Ar]^{2+}$ (Figure S7) should be observable, however we did not detect these species in any of our experiments with tagged ArI, perhaps due to repulsion of extra charge on the complex. So the same experiment was performed under the same conditions with neutral phenyl iodide, hoping to detect theses specie. Interestingly, $[PdL_2Ph]^+$ along with $[PdL_2PhI]K^+$ (oxidative addition of PhI to the Pd(0)) were observed confirming the involvement of this active specie in the mechanism (Figure S8). Using a different neutral aryl iodide, 4-idodanisole, gave analogous results.
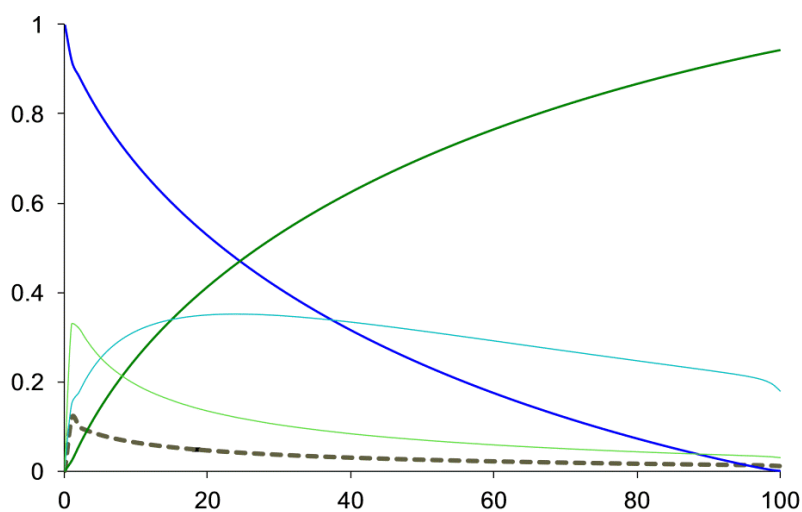
Figure S7: Simulated graphs for hydrodehalogenation in MeOH. Gray dashed line represents the trend of expected $PdL_2Ar(MeOH)^{+2}$.
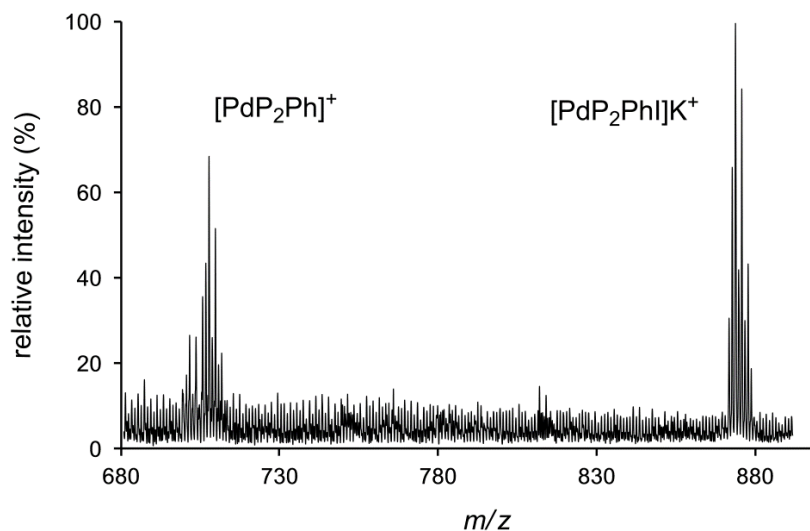
Figure S8 Figure S6. Isotope patterns of $[PdL_2PhI + K]^+$ and $[PdL_2Ph]^+$. Average of over 500 spectra over the course of the reaction.

Enthalpy and entropy of activation

The reaction was repeated at four different temperatures (306.2, 307.6, 316.5 and 339.6 K) to allow the measurement of $\Delta H^{\ddagger} = 72 \pm 8$ kJ mol^{-1} and $\Delta S^{\ddagger} = -60 \pm 170$ J mol^{-1} via the construction of an Eyring plot (below). The large error in the entropy of activation is due to the fact that at the low concentrations used in these experiments (0.5 mM), getting the near-perfect data required for measuring a precise intercept in practice is very difficult.

$$y = -8634.4x + 15.911$$
$$R^2 = 0.9782$$
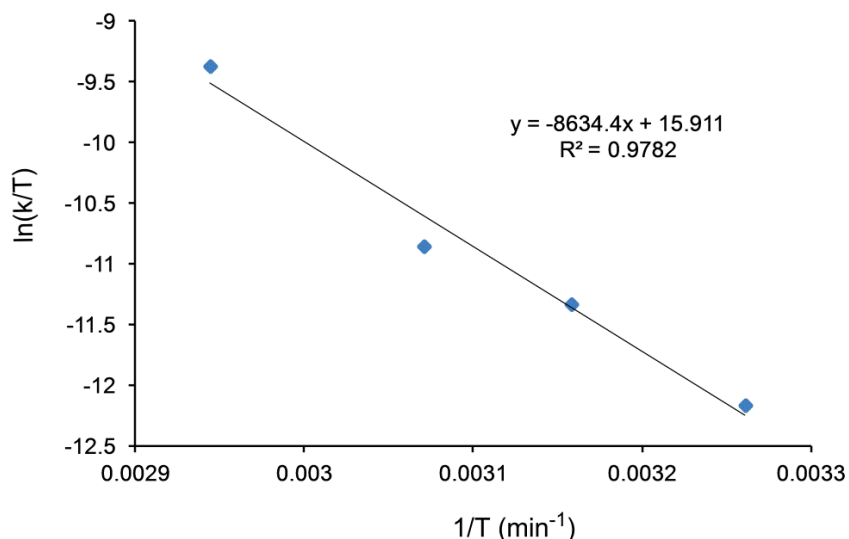
Figure S9: Eyring plot of hydrodehalogenation in MeOH.

Homocoupling reaction as the side-cycle

The appearance of the PdP$_2$Ar$_2$ intermediate is interesting; it grows in slowly throughout the reaction and starts to goes away only very slowly once about half of the ArI is consumed. In cross-coupling reactions we have studied involving formation of biphenyls [Ahmadi Z., Logan J., Wu W., Oliver A. G., McIndoe J. S., *submitted*] reductive elimination of the product is very fast, suggesting that the high abundance of this intermediate throughout implies that it is the *trans* rather than the *cis* product. As it is observed the abundance of PdP$_2$Ar$_2$ reaches even more than the combination of both active intermediates at maximum, but it only produces about 2% Ar-Ar overall.
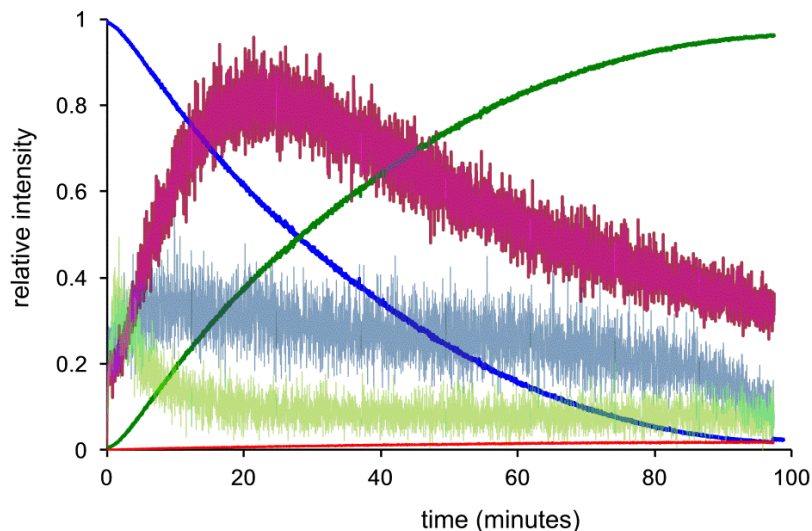
Figure S10: Normalized relative abundance of PdP$_2$Ar$_2$ and ArH in the reaction in MeOH in comparison with other intermediates, ArI and ArH.

MS/MS allows us to easily probe this assumption, by subjecting the ion to collision-induced dissociation (CID). If the two groups are cis to one another, we would expect the reductive elimination of Ar-Ar to be facile. The PdP$_2$(Ar)(H) ion, for example, cleanly eliminates ArH (at *m/z* 353) even at low voltages (below 10V) and at higher voltage, 20V, ArH is the most dominant fragment. Conversely, the PdP$_2$Ar$_2$ ion (a doubly charged ion at *m/z* 668) decomposes incoherently to a range of fragments, including [PPh$_4$]$^+$ (*m/z* 339), [Pd(Ar)(CHPPh$_3$)]$^+$ (*m/z* 733) but only a very small amount of [Ar-Ar]$^{2+}$ (at *m/z* 352).
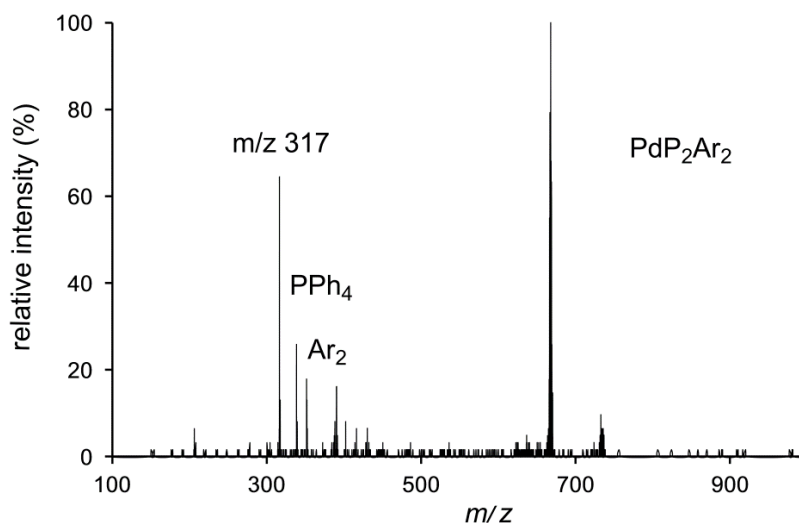
Figure S11: MS/MS on *m/z* 668. Average of 12 spectra at voltages between 15-20V.

11
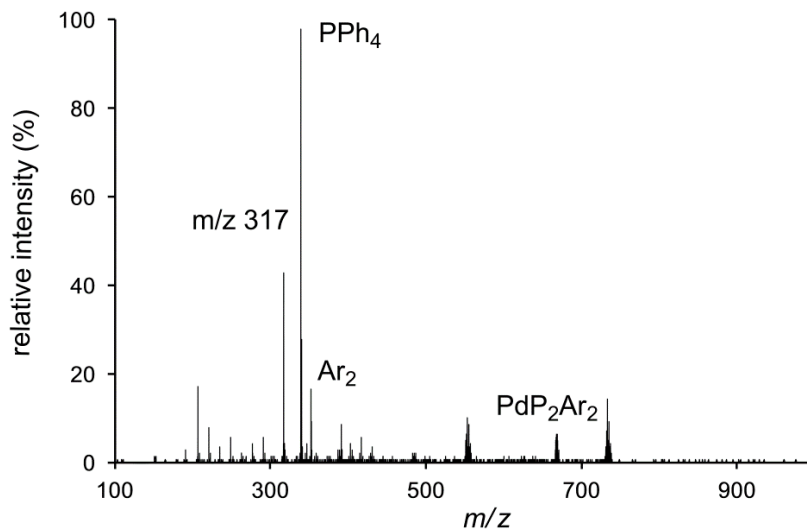
Fig S12. MS/MS of *m/z* 668. Average of 16 spectra at voltages lower than 10 V.
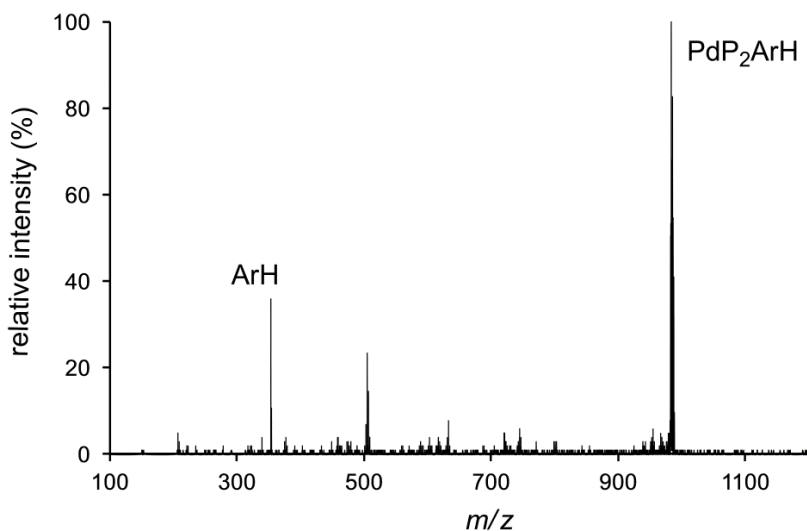
Fig SI13. MS/MS on *m/z* 983. Average of 17 spectra at voltages lower than 10V.
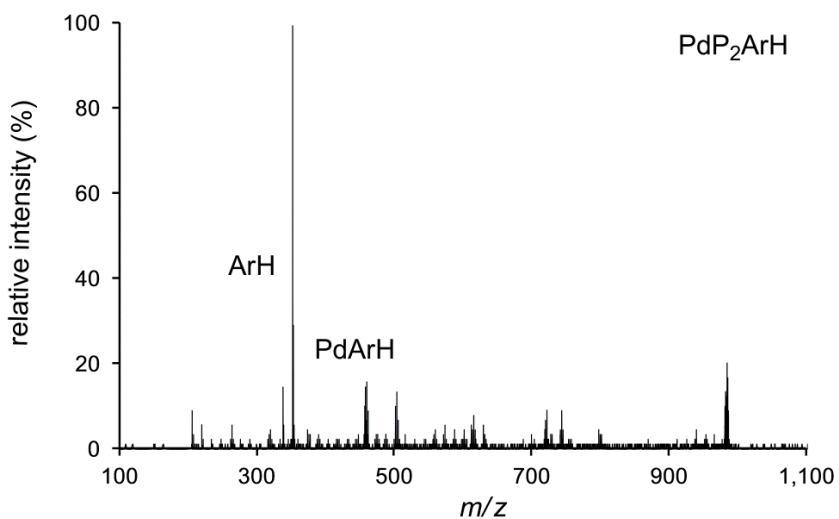
Fig S14. MS/MS on *m/z* 983. Average of 30 spectra at voltages between 15-20.

12

References

1. K. L. Vikse, Z. Ahmadi, C. C. Manning, D. A. Harrington and J. S. McIndoe, *Angew. Chem. Int. Ed.*, 2011, **123**, 8454-8456.

2. "Powersim Studio 9 | Powersim Software." 21 Jan. 2013 <http://www.powersim.com/>